Effect of group-based vs individualized stimulation site selection on reliability of network-targeted TMS

Arianna Menardi [a,b,*], Recep A. Ozdemir [c], Davide Momi [c,d], Ehsan Tadayon [c], Pierre Boucher [c], Antonino Vallesi [b], Alvaro Pascual-Leone [e,f,g], Mouhsin M. Shafi [c], Emiliano santarnecchi [a,**]

[a] Precision Neuroscience & Neuromodulation Program, Gordon Center for Medical Imaging, Department of Radiology, Massachusetts General Hospital, Harvard Medical School, Boston, MA, USA
[b] Department of Neuroscience & Padova Neuroscience Center, University of Padova, Padova, Italy
[c] Berenson-Allen Center for Noninvasive Brain Stimulation, Department of Neurology, Beth Israel Deaconess Medical Center, Harvard Medical School, Boston, USA
[d] Department of Neuroscience, Imaging and Clinical Sciences, University "G. d'Annunzio", Chieti, Italy
[e] Department of Neurology, Harvard Medical School, Boston, MA, USA
[f] Hinda and Arthur Marcus Institute for Aging Research and Deanna and Sidney Wolk Center for Memory Health, Hebrew SeniorLife, Rosindale, MA, USA
[g] Guttmann Brain Health Institut, Barcelona, Spain

ARTICLE INFO

ABSTRACT

Background: Transcranial magnetic stimulation (TMS) is a widely used technique for the noninvasive assessment and manipulation of brain activity and behavior. Although extensively used for research and clinical purposes, recent studies have questioned the reliability of TMS findings because of the high inter-individual variability that has been observed.

Objective: In this study, we compared the efficacy and reliability of different targeting scenarios on the TMS-evoked response.

Methods: 24 subjects underwent a single pulse stimulation protocol over two parietal nodes belonging to the Dorsal Attention (DAN) and Default Mode (DMN) Networks respectively. Across visits, the stimulated target for both networks was chosen either based on group-derived networks' maps or personalized network topography based on individual anatomy and functional profile. All stimulation visits were conducted twice, one month apart, during concomitant electroencephalography recording.

Results: At the network level, we did not observe significant differences in the TMS-evoked response between targeting conditions. However, reliable patterns of activity were observed— for both networks tested— following the individualized targeting approach. When the same analyses were carried out at the electrode space level, evidence of reliable patterns was observed following the individualized stimulation of the DAN, but not of the DMN.

Conclusions: Our findings suggest that individualization of stimulation sites might ensure reliability of the evoked TMS-response across visits. Furthermore, individualized stimulation sites appear to be of foremost importance in highly variable, high order task-positive networks, such as the DAN.

1. Introduction

In recent years, growing interest has been directed toward the understanding of the tight link between neural processes and human behavior. In the past, this has largely been accomplished thanks to neuroimaging and electrophysiological studies, which however suffer from the major shortcoming of being able to show correlation, but not causality, between neural events and behavioral outcomes. One possible approach for the study of cause/effect relationships is represented by non-invasive brain stimulation (NiBS) approaches, especially transcranial magnetic stimulation (TMS) (Hallett, 2000). TMS relies on the laws of electromagnetism, whereby when an electric current travels through a coil of wires, a strong magnetic field is generated, capable of inducing a perpendicular, secondary electrical field in an underneath medium (Hallett, 2000). When applied to the brain, this principle has hence been used to induce externally caused neural discharges. Furthermore, because our brain is a plastic system, TMS can be employed to favor mechanisms resembling those of long-term potentiation or depression

(Huerta and Volpe, 2009). Since TMS represents a safe and noninvasive approach, several stimulation devices and protocols have received the Food and Drug Administration (FDA) approval for the treatment of medication-resistant Depression (Connolly et al., 2012), Migraine (Schwedt and Vargas, 2015), Obsessive Compulsive Disorder (Stultz et al., 2020) and smoking cessation (Young et al., 2021). However, beyond that, most other TMS protocols have only reached a level B evidence (probable efficacy) for the treatment of specific symptoms in other pathologies, such as stroke, fibromyalgia, multiple sclerosis, Parkinson's disease and posttraumatic stress disorder (Lefaucheur et al., 2020). A major concern to TMS applications is the consistency and replicability of its findings due to the high inter-subject variability (Lopez-Alonso et al., 2014; Nettekoven et al., 2015; Terranova et al., 2019; Belardinelli et al., 2019; Corp et al., 2021; Valero-Cabrè et al., 2017). Apart from dosing and stimulation parameters, another important source of variability is the selection of the stimulation sites, which in most studies is chosen based on approximate anatomical landmarks (e.g. based on the 10–20 electroencephalography-EEG system, or the "5 cm rule" for the selection of dorsolateral prefrontal areas). Indeed, most TMS studies use anatomical coordinates derived from common brain templates to determine stimulation spots in non-motor regions with an implicit assumption that a given anatomical region in the cortex is part of the same network or involved in the same brain function across individuals. Considering the extensive variability in individual brain morphology especially within higher order associative/heteromodal cortices (Doucet et al., 2019) further transformation of these average brain coordinates into individual MRI space makes it hardly possible to target functionally identical cortical nodes across subjects and most probably contributes to variability in TMS evoked brain responses derived from non-motor brain regions (Ozdemir et al., 2021). This results in poor consistency of the stimulated areas across study participants, which can be largely overcome by means of more personalized approaches, for example relying on the combination of TMS and neuroimaging data for individual target selection. In the past years, this has been a hot topic across research groups, proving how individualized, network-based approaches might enhance the efficacy of circuit-based interventions (Nestor and Blumberger, 2020), both in healthy young participants (Ozdemir et al., 2020), as well as in pathological population, such as patients suffering from Depression (Cash et al., 2020; Moreno-Ortega et al., 2020; Siddiqi et al., 2020). Furthermore, recent evidence points in the direction of brain functional patterns to represent unique signature of the individual brain (Finn et al., 2015), and so the evoked responses to TMS to be highly individual-specific (Ozdemir et al., 2021). Although greater consistency in stimulation targets might not be directly linked to greater therapeutic efficacy, consistency across TMS studies might be achieved via individualized target selection by taking into account the underlying, highly variable, brain structural and functional pathways reported to affect neuronal response propagation patterns to TMS (Momi et al., 2021). Indeed, previous studies have reported the reliability of the induced responses following individualized, neuronavigated, TMS applied to dorsolateral prefrontal or motor areas (Lioumis et al., 2009). Similarly, the strongest behavioral effect sizes have been reported in studies employing personalized TMS targeting based on functional magnetic resonance imaging (fMRI) connectivity, compared to studies employing targeting based on structural, population-derived coordinates or EEG electrodes positions (Sack et al., 2009). Differently from prior studies (see for example (Ozdemir et al., 2020; Lioumis et al., 2009)), here we aimed at assessing the efficacy and reproducibility of the induced response across different scales (network and electrode level) comparing different degrees of personalized stimulation. To address this, we compared the amount of induced activity and test-retest reliability to a single pulse TMS protocol targeting either i) group-derived, generic stimulation targets (g) or ii) personalized sites based on the individual functional neuroimaging data (i). In particular, group-based versus individualized targeting was assessed on two resting state networks: the Dorsal Attention (DAN) and Default Mode

(DMN) Networks. The efficacy of the different stimulation protocols was measured in terms of the induced activity recorded in the surrounding electrodes, as well as in spatially defined network maps. Furthermore, the reliability across visits of such measures was also compared. We chose the right superior parietal gyrus (SPG) and the right angular gyrus (ANG) as targeting points for the stimulation of the DAN and DMN respectively. The definitions of such targets on the cortex was achieved either via a group-derived (atlas-based) network maps morphed on the individual anatomy (for the g condition), or by means of data-driven seed-to-voxel analyses (for the i condition). As a result, different network maps were employed to individuate the stimulation target and for the subsequent analysis of the TMS-EEG response. We hypothesized that stimulation of functionally individualized network nodes would result in better network engagement (i.e., efficacy of stimulation in activating the targeted network); as well as higher reliability of such measure. Indeed, TMS coil placement is usually based on either anatomical target or based on group-derived functional network maps. However, this latter approach can inadvertently target different functional networks, due to the fact that networks' spatial distribution is highly variable across subjects, yet reliable within (Oathes et al., 2021), such as that different networks may occupy the same anatomical location across subjects (Gordon et al., 2017; Lynch et al., 2022). On the other hand, more precise targeting can be achieved when considering the individual functional connectivity profile (Lynch et al., 2022). Indeed, recent literature suggests that, if our aim is to stimulate an individual brain area, stimulation targets based on the individual functional connectivity to that area increase our chances of reliably target it (Oathes et al., 2021). Our rationale was hence that the readout of the induced activity in a network following its individualized targeting should be a more solid estimate, especially across visits, of its true state of activation, compared to what measured from a general parcellation scheme following stimulation of a general target. Hence, individualized stimulation based on functional connectivity should allow us to more reliably target the desired individual network across visits (Oathes et al., 2021)

Finally, because individualized targeting inevitably brings the need to address the cost/benefits ratio, we further compared the efficacy and reliability of two different degrees of personalization in a small subsample of our participants. This was achieved by assessing whether individualization based on identifying network topographies/maps using independent component analyses (ICA) approach for each subject would further enhance stimulation efficacy and reliability. This check is necessary to determine if individualized protocols, that are necessarily more expensive and time consuming, are worth in face of simpler and more straightforward approaches.

2. Methods

2.1. Participants

Based on prior published work (Lioumis et al., 2009; Sack et al., 2009; Kerwin et al., 2018), a sample size of 24 healthy participants (16 males, age = 29.67 ± 10.6 years, range 19–49 years old) was employed in this study. Written informed consent was obtained from each participant prior to volunteering. The study was approved by the Beth Israel Deaconess Medical Center Review Board and conducted in line with the Declaration of Helsinki.

2.2. Neuroimaging data acquisition and preprocessing

All subjects underwent the acquisition of structural and functional magnetic resonance imaging (rs-fMRI) data for the identification of the individual resting state networks to stimulate. On a 3T GE Healthcare scanner, T1-weighted anatomical data (repetition time (TR)= 6.9 ms, echo time (TE)= 2.9 ms, voxel-size= $0.937 \times 0.937 \times 1$ mm^3, flip angle (FA)= 15 deg., field of view (FOV)= 240 mm, number of volumes= 166, duration= 7.2 min), and T2* rs-fMRI data (TR= 3.196 ms,

TE= 25 ms, voxel size= 1.87 × 1.87 × 2.5 mm³, FA= 90 deg., FOV= 240 mm, duration= three runs lasting 5 min each) were acquired. Rs-fMRI data were then preprocessed by means of FMRIPREP (vl.2). In more detail, anatomical data underwent spatial normalization, brain extraction and tissue segmentation into white matter, gray matter and cerebrospinal fluid components. Functional scans were slice-timing and motion corrected; furthermore, functional timeseries were bandpass filtered (0.008–0.08) and underwent the regression of physiological noise by means of CompCor. Resting state functional networks were then identified based on the Yeo's seven networks parcellation (Yeo et al., 2011). A detailed description on how individualized functional networks were derived is available in the Supplementary Materials, as well as in a recent work by some of the authors (Ozdemir et al., 2020).

2.3. TMS protocol and network targets identification

Following neuroimaging data acquisition, participants underwent a single pulse TMS protocol (MagPro X-100 stimulator by MagVenture A/S) consisting of 120 monophasic posterior-to-anterior waveform pulses (per condition, per visit, tot=480 pulses) at an intensity of 120% of the individual resting motor threshold (RMT). RMT was defined as the smallest machine output intensity capable of inducing a Motor Evoked Potential (MEP) of at least 50 uV peak-to-peak amplitude in 5/10 trials. MEPs were recorded by means of Ag-AgCl surface electrodes placed on the first dorsal interosseous (FDI) and abductor pollicis brevis (APB) muscles of the right hand, with the ground electrode placed on the right ulnar styloid process. Individual RMT are reported in table S1 in the Supplementary Materials. TMS pulses were delivered on the participants' scalp via neuronavigation of the individual T1w image (imported in the Brainsight TMS frameless neuronavigation system), which was coregistered to digitalized landmarks for online monitoring of the head and coil position. During the entire TMS session, concomitant EEG recording was performed via a TMS-compatible amplifier (actiCHamp system, Brain Products GmbH). A 64 channels cap was used, labeled according to the 10–20 EEG system. EEG data were referenced to Fp1, sampled at 1000 Hz and their position on the scalp coregistered to the individual MRI by means of Brainsight TMS frameless neuronavigation system. Electrode FPz was used as ground. The recorded TMS-EEG data were preprocessed via a home-based script running in Matlab 2017b (MathWorks Inc.), relaying on EEGLAB (Delorme and Makeig, 2004) functions and TESA Toolbox for artifact removal (Rogasch et al., 2017). Briefly, EEG preprocessing steps included baseline correction considering the 500 ms precedent to the pulse, removal of noisy channels and epochs (of 1500 ms each) based on visual inspection, voltage (≥100 uV), kurtosis (≥3) and joint probability (single channel-based threshold ≥3.5 SD). The TMS artifact was removed by means of zero-padding (−2 ms to 14 ms time window) and a fast ICA (fICA) inspection. Before that, data were reduced into 60 components by means of principal component analysis (PCA) to minimize the risk of overfitting. EEG data were then interpolated around the zero-padding time window, band pass filtered (1–100 Hz), notch filtered (57–63 Hz) and referenced to global average. A second round of PCA and fICA were performed to remove additional sources of noise (eye movements, muscle, cardiac and electrodes noise, auditory evoked potentials). Finally, data were low pass filtered (<50 Hz) and signal from missing channels eventually interpolated. Additional information on the TMS-EEG recording parameters, preprocessing, as well as few exemplificative plots of the induced activity can be found in the Supplementary Materials and in a prior publication by some of the authors (Ozdemir et al., 2020). The right SPG and the right ANG gyri were chosen as stimulation sites for the targeting of the DAN and the DMN network respectively (Fig. 1A, B). For our group-based approach, the confidence maps from a sample of 1000 healthy individuals (Yeo et al., 2011) were morphed via Freesurfer spherical registration into the individual anatomy and the point of maximum confidence chosen as target (Fig. 1A). For our individualized approach, the site of stimulation was instead chosen by means of a seed-based approach, which was iteratively performed starting from each node of the network of interest, until the SPG and ANG could be identified respectively (Fig. 1A)
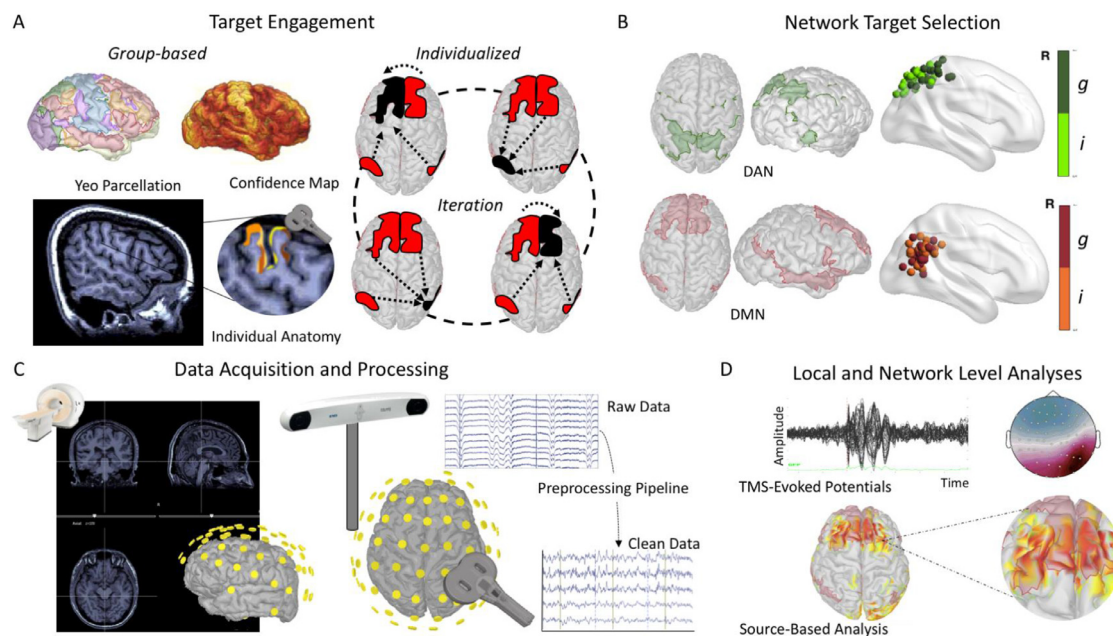

Fig. 1. Methodological Workflow and Measures of Interest. A. Group-based stimulation targets were defined based on the confidence map derived from 1000 participants (Yeo et al., 2011), which were then morphed to the individual anatomy. Alternatively, individualized stimulation targets were derived by means of an iterative seed-based approach. **B.** Efficacy and test-retest reliability were assessed following network-targeting of the DAN and DMN. Interindividual differences based on target selection for the group vs individualized approach are shown. **C.** Individual neuroanatomy was used for both target selection and neuronavigation purposes during concomitant TMS-EEG. All visits were repeated 1 month apart. **D.** The efficacy and reliability of the stimulation was assessed in terms of the induced activity at the source level. Furthermore, the amount of induced activity and its reliability was also assessed at the electrode level, looking at the average response in the electrodes surrounding the stimulation site.

(see Supplementary Materials for more details on the procedure). Furthermore, a small subsample of our participants ($n = 10$) underwent a third stimulation condition, where the stimulation target was identified on entirely data-driven network maps. In this case, ICA was performed over the 3 runs of rs-fMRI and the local maxima of the SPG and ANG were identified by one of the experimenters. The order of stimulation between targeting conditions (*g, i, ica*) and targeted networks (DAN, DMN) was randomized. All stimulation visits were then repeated after one month. Notably, the stimulation site was identified based on the individual rs-fMRI at baseline and it was then targeted across the test-retest visits. Prior literature studies have highlighted that the individual intrinsic connectivity profile, especially at rest, is reliable and consistent across separate visits and days (Cash et al., 2020; Finn et al., 2015; Fox et al., 2013). Furthermore, clinical practice often limits the possibility to have more than one scanning acquisition, such as that the few TMS studies relying on fMRI-derived stimulation sites have also identified the stimulation hotspot based on a single MRI session (for a review see (Cash et al., 2020)). Despite the promising results of such studies on individualized targeting over sham or general targeting conditions, there is not yet evidence of the replicability of the underlying evoked response by the stimulation, which we aim to address in this study.

2.4. Network and electrode-level analyses

In our first set of analyses, we compared the efficacy and the reliability of the induced changes in source-level activity following stimulation of either the DAN or DMN network. In order to do so, TMS induced activity was reconstructed at the source level by means of the Brainstorm toolbox (Tadel et al., 2011). Anatomical data and TMS-EEG recordings of each participant were imported to allow source reconstruction to be carried out on the individual brain. The inverse problem was approached using the minimum norm estimation, where a measure of the induced current at each vertex is computed in the form of current density map. In this regard, dipoles are built perpendicular to the imported cortical surface of the individual, based on the notion that pyramidal neurons are organized in columns normal to the outer cerebral layer (Tadel et al., 2011). Baseline recordings (500 ms) prior to pulse delivery were used as noise covariate to normalize the data in form of z-score. Furthermore, the scalp-to-cortex distance and the induced normalized electric field were computed by means of SimNIBS v3.2.6 (www.simnibs.org) to control for the possibility that differences in the induced activity between stimulation conditions were not due to differences in the amount of stimulation reaching the brain (see Supplementary Materials).

To measure the induced effect in the resting state networks, EEG activity was extracted from six scouts, defined as regions of interest, or set of dipoles, on the individual cortical surface. Each scout was specific to the type of stimulation performed and represented the network map used to identify the stimulation target in each condition. In more details: in the group-based condition, each scout represented the DAN and DMN resting state networks of the Yeo parcellation (Yeo et al., 2011); in the individualized condition, DAN and DMN maps were reconstructed based on an iterative seed based approach; finally, in the *ica* stimulation condition, DAN and DMN maps were entirely data-driven from ICA analysis of the individual fMRI. All timeseries were corrected based on the individual baseline and transformed into z-scores.

Secondarily, we also checked for the efficacy and reliability of the induced response at the electrode level. In this case, we identified the six electrodes closer to the stimulation site based on their Euclidian distance. Their activity was averaged to obtain a single time series, which was further normalized in respect to the baseline activity, consisting of the 500 ms before pulse delivery. According to the 10–20 EEG system, the electrodes closer to the DAN stimulation sites corresponded to CP2, P2, Pz, CP4, P4, PO4 and those closer to the DMN stimulation site corresponded to CP6, P6, C6, CP4, P4 and PO4.

To determine the efficacy and reliability of stimulation, we computed the amount of induced activity as the area under the curve (AUC) in

the whole 500 ms post pulse, as well as across ten consecutive, non-overlapping, temporal windows, consisting of 50 ms each, from the time of the pulse to 500 ms post pulse. This allowed us to determine if a significant effect was present on a sufficiently large temporal window after the pulse, as well as to characterize where, in terms of smaller windows after the pulse, the induced activity was maximum and most reliable. Within-group, paired sample t-tests were run to compare the induced activity to baseline. Within subject two-way repeated measures Analysis of Variance (rm-ANOVA) were run to test if there was any difference in the AUC between stimulations conditions, visits and their interaction. A significant threshold was set at $\alpha = 0.05$ to reject the null hypothesis. To control for the risk of multiple comparisons, Bonferroni correction was applied to the paired sample t-tests; whereas the Tukey-Kramer test was applied to the rm-ANOVA models.

To determine the reliability of the induced TMS response following the group-based versus individualized stimulation conditions, we ran intra class correlation (ICC) in Matlab 2017b (MathWorks Inc.). First, for each stimulation condition (*g, i* and *ica* for the DAN and DMN stimulation), the AUC in the time window following the pulse at V1 and V2 were computed. To measure the degree of absolute agreement between the measures, ICC was computed based on a one-way random effects model of type 1–1 (McGraw and Wong, 1996; Koo and Li, 2016) with the significant threshold set at $p < 0.05$. To correct for multiple comparisons and thus the risk of incurring into false positive findings, the obtained AUC values were randomly shuffled 1000 times and their reliability, assessed with ICC in each iteration, compared with the ICC values obtained from the real V1 and V2 correlation. As such, we generated a null distribution of ICCs based on the permutation analyses and we re-compute the significance of original ICC (p-values) by calculating the probability of its magnitude (r values) in the null distribution. Finally, an ICC value (r values) in the original analyses is considered to survive permutation, and thus significant, only if the magnitude of a given original ICC is above 95% of all magnitudes derived from permutation tests. In other words, we were interested in assessing if the magnitude of the correlation between V1 and V2 for each condition (*g, i, ica*) was higher than correlations occurring by chance, as tested via the random shuffling among their measurements over 1000 times. The same analyses were run both in the i) 500 ms time window following the pulse, as well as in ii) non-overlapping windows, obtained by diving the 500 ms in ten separate smaller windows of 50 ms each. Compared to other correlational approaches, ICC has the advantage of operating on data organized in groups, rather than as paired observations, whereby the data are scaled based on a pooled mean and standard deviation, thus making it the desirable statistical approach for the study of reproducibility and consistency of the same measurements across observations.

3. Results

3.1. Efficacy of stimulation at the network level

Paired sample t-tests were run to compare the mean difference between the baseline and the induced activity across conditions and visits. At both V1 and V2, stimulation of the DAN resulted in a significant difference from baseline for both for the *g* (V1: $t_{(22)} = -6.41$, $p < 0.0001$, Hedges' $g = 1.36$; V2: $t_{(22)} = -8.18$, $p < 0.0001$, Hedges' $g = 2.06$) and *i* (V1: $t_{(21)} = -5.02$, $p < 0.0001$, Hedges' $g = 1.18$; V2: $t_{(21)} = -4.89$, $p < 0.0001$, Hedges' $g = 1.28$) stimulation conditions. Following stimulation of the DMN, significant difference from baseline was observed across visits for the *g* (V1: $t_{(21)} = -6.76$, $p < 0.0001$, Hedges' $g = 1.77$; V2: $t_{(21)} = -7.3$, $p < 0.0001$, Hedges' $g = 1.76$) and *i* (V1: $t_{(22)} = -6.95$, $p < 0.0001$, Hedges' $g = 1.41$; V2: $t_{(22)} = -7.39$, $p < 0.0001$, Hedges' $g = 1.63$) conditions.

All the results survived Bonferroni correction ($0.05/8$; $\alpha = 0.0062$). Fig. 2 reports the bar charts for stimulation visits and conditions, highlighting the results surviving the Bonferroni correction.
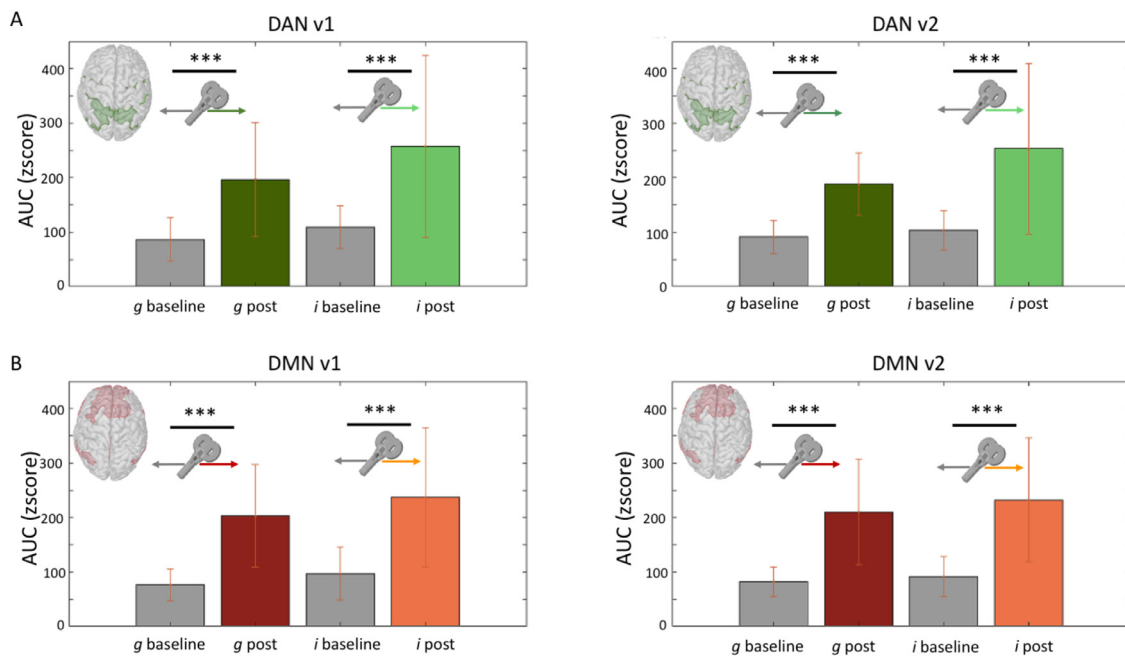
Fig. 2. Induced source activity compared to baseline. A. Following stimulation of the DAN, a significant difference from baseline was observed for both the group-based and the individualized condition. Both stimulation scenarios were capable of inducing significantly higher activity (AUC in the 500 ms post pulse) compared to baseline at both test and retest visits. **B.** Similarly for the DMN condition, a significant difference from baseline was observed following both the group-based and the individualized stimulation. Significant difference from baseline was observed across visits. All significant comparisons survived the Bonferroni correction (*** $p<0.0001$). Bars represent standard deviations from the mean. (For interpretation of the references to colour in this figure legend, the reader is referred to the web version of this article.)

Next, we compared the AUC following the stimulation of group-based versus individualized targeting. Although for both networks a slightly higher activity was observed following the i stimulation compared to the g stimulation condition, within subject two-way rmANOVA revealed no differences across stimulation conditions and visits for either the DAN ($F_{(1,21)=}$ 2.97, $p = 0.1$, Hedges' g V1= 0.4, Hedges' g V2= 0.52) or the DMN ($F_{(1,21)}= 1.24$, $p = 0.28$, Hedges' g V1= 0.28, Hedges' g V2= 0.13) (Fig. 3). Similarly, when the induced activity was analyzed in ten separate non-overlapping windows, no significant results emerged when comparing between stimulation conditions.

3.2. Reliability of the evoked response at the network level

The reliability of the two stimulation conditions was assessed by means of ICC over 1000 permutations, comparing the AUC in the whole window (500 ms) post pulse across visits, as well as by means of consecutive, non-overlapping windows of 50 ms each. In other words, we were interested in assessing if the magnitude of the correlation between V1 and V2 for each condition (g and i) was higher than correlations occurring by chance, as tested via the random shuffling among their measurements over 1000 times.

For the DAN network (Fig. 4A), the induced activity following the g stimulation condition in the 500 ms post pulse was not observed to be reliable (ICC=0.51, p_{corr}=0.06). Analyses on the single time windows resulted in a significant intra class reliability only in the 200–250 ms time-window post pulse (ICC= 0.67, p_{corr}= 0.04). Significant ICC values were also observed in the first 50 ms post pulse (ICC= 0.47, $p = 0.01$), as well as in the 50–100 ms (ICC= 0.35, $p = 0.048$), 100–150 ms (ICC= 0.58, $p = 0.001$) and 400–450 ms (ICC= 0.39, $p = 0.03$) time-windows, which however did not survive the permutation correction.

On the other hand, high reliability was observed in the entire 500 ms post pulse for the i stimulation condition (ICC=0.83, p_{corr}=0. 004). Analysis of the single time-windows revealed a significant pattern at 50–100 ms (ICC= 0.50, p_{corr}= 0.04), 100–150 ms (ICC= 0.79, p_{corr}= 0.03), 150–200 ms: (ICC= 0.5, p_{corr}= 0.04), 250–300 ms (ICC= 0.86, p_{corr}=

0.02), 300–350 ms (ICC= 0.56, p_{corr}= 0.01) and 450–500 ms (ICC= 0.77, p_{corr}= 0.04). In the 350–400 ms ($p = 0.045$) and 400–450 ms (ICC= 0.38, $p = 0.03$) time-windows, ICC values did not survive the permutation correction.

Similarly for the DMN network (Fig. 4B), the g condition resulted in poor reliability of the response in the whole 500 ms post pulse (ICC=−0.13, p_{corr}=0.7). At the level of the single time-windows, a significant ICC value was observed only at 150–200 ms (ICC= 0.46, $p = 0.01$), which however did not survive the permutation correction.

On the other end, reliability across visits was observed following the i stimulation condition (ICC=0.57, p_{corr}=0.03). At the single time-windows level, high reliability was observed at 250–300 ms (ICC= 0.78, p_{corr}= 0.02) and at 300–350 ms post pulse (ICC= 0.54, p_{corr}= 0.044). In addition, significant ICC values for the i condition were also observed in the first 50 ms post pulse (ICC=0.51, $p = 0.005$), which however did not survive the permutation correction.

3.3. Efficacy of stimulation at the electrode level

Paired sample t-tests were run to compare the mean difference between the baseline versus the induced activity across conditions and visits. For the DAN condition, a significant difference from baseline was observed across visits for both the g (V1: $t_{(21)}= −6.7$, $p<0.000$, Hedges' $g = 1.39$; V2: $t_{(21)}= −5.98$, $p<0.0001$, Hedges' $g = 0.84$) and i (V1: $t_{(21)}= −6.27$, $p<0.0001$, Hedges' $g = 1.54$; V2: $t_{(21)}= −7.75$, $p<0.0001$, Hedges' $g = 1.8$) stimulations (Fig. 5A). For the DMN condition, a significant difference was observed across visits for both the g (V1: $t_{(21)}= −5.54$, $p<0.0001$, Hedges' $g = 1.22$; V2: $t_{(21)}= −6.86$, $p<0.0001$, Hedges' $g = 1.44$) and i stimulations (V1: $t_{(22)}= −6.98$, $p<0.0001$, Hedges' $g = 1.16$; V2: $t_{(22)}= −4.78$, $p<0.0001$, Hedges' $g = 1.04$) (Fig. 5B). All contrasts survived the Bonferroni correction (0.05/8; $\alpha = 0.0062$).

For each network and time-window, a two-way rmANOVA was run to test if there was any difference in the AUC between stimulations conditions, visits and their interaction.
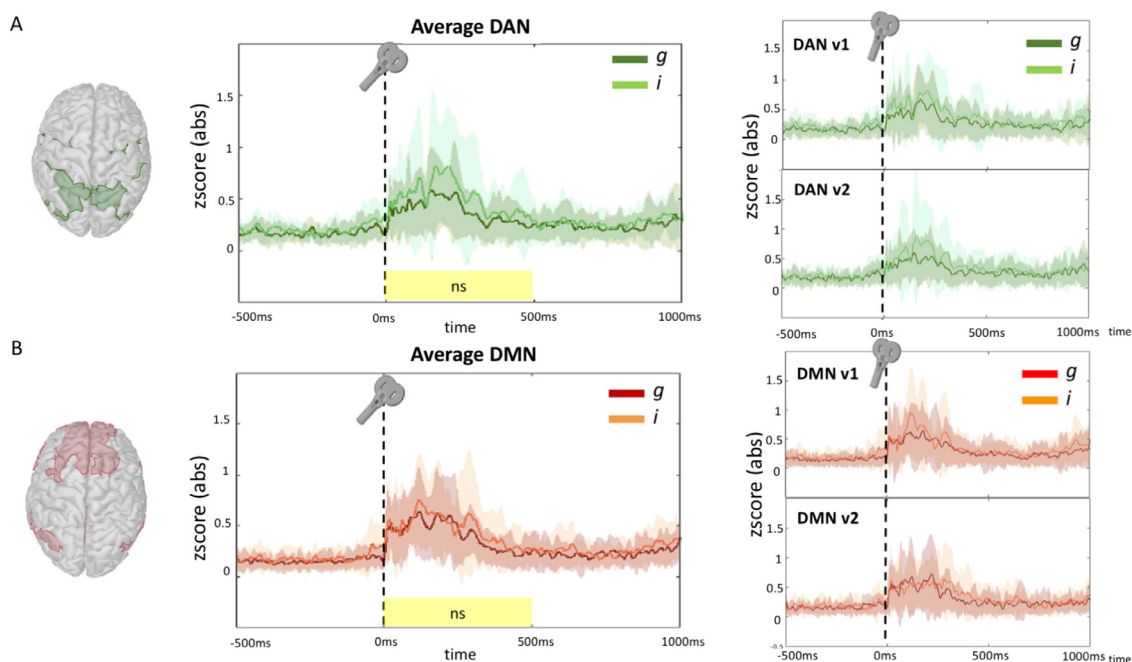
Fig. 3. Efficacy of group-based versus individualized stimulation at the network level. The AUC computed from the timeseries extracted from the DAN and DMN network maps was compared between the group-derived and individualized targeting condition. **A.** Following stimulation of the DAN, no significant difference was observed between the *g* and *i* condition. **B.** Following stimulation of the DMN, no significant difference was observed between the *g* and *i* condition. The yellow shaded area represented the first 500 ms post pulse where the analyses were conducted. (For interpretation of the references to colour in this figure legend, the reader is referred to the web version of this article.)
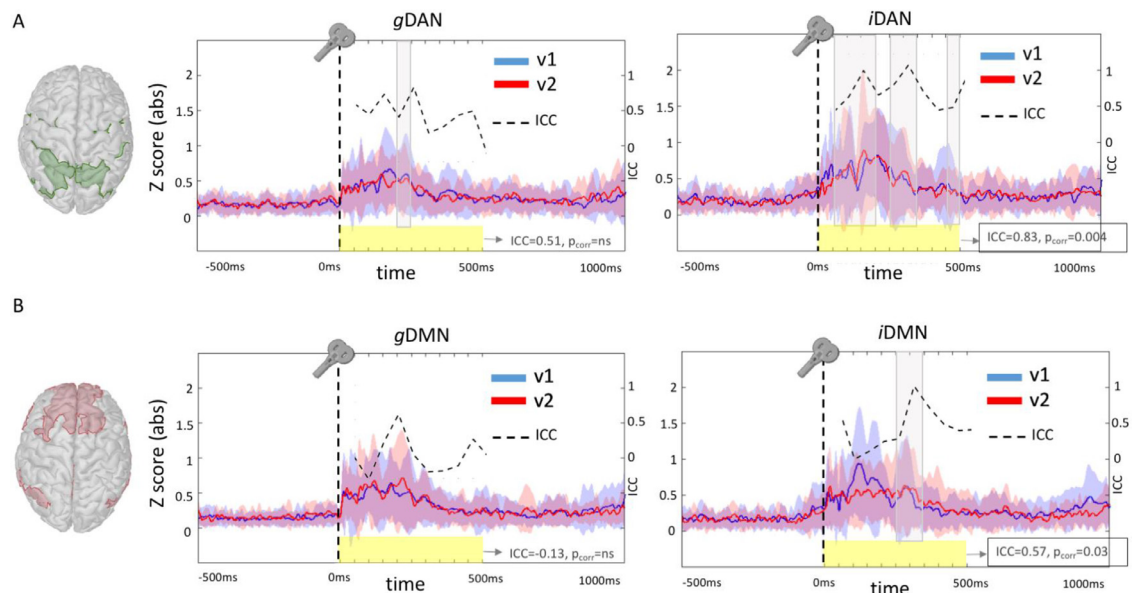

Fig. 4. Reliability of the evoked response following group-derived or individualized stimulation. A. For the DAN, higher reliability across visits was observed following the *i* stimulation condition, compared to the *g* stimulation condition. Significant reliability was observed throughout the entire 500 ms post pulse, as well as in the 50–100 ms, 100–150 ms, 150–200 ms, 250–300 ms, 300–350 ms and 450–500 ms time windows. **B.** Similarly for the DMN condition, evidence of reliability across visits was observed following the *i* stimulation. Significant reliability was observed across all the 500 ms post pulse and specifically at 250–300 ms and 300–350 ms post pulse. The yellow shaded area represented the first 500 ms post pulse where the analyses were conducted. The gray shaded area represents the time-windows where reliability of the response surviving the permutation correction was observed. (For interpretation of the references to colour in this figure legend, the reader is referred to the web version of this article.)

For the DAN network (Fig. 6A), no significant effect across stimulation conditions, visits and their interaction was observed on the whole 500 ms post pulse period (Hedges'g V1= 0.03, Hedges'g V2= −0.14). When analyses were re-run on the single time-windows, a significant effect of visit was observed at 300–350 ms ($F_{(1,21)}$=4.42, $p = 0.047$) and 350–400 ms ($F_{(1,21)}$=5.08, $p = 0.035$). Post hoc comparison revealed a

slightly higher mean difference activity (Mdiff) at V2 compared to V1 (300–350 ms: Mdiff= 4.3e-06, $p = 0.047$; 350–400 ms: Mdiff= 5.7e-06, $p = 0.035$).

In the DMN condition (Fig. 6B), a significant effect across stimulation conditions was observed on the whole 500 ms post pulse time window($F_{(1,21)}$=5.45, $p = 0.03$, Hedges'g V1= 0.06, Hedges'g V2= 0.54).
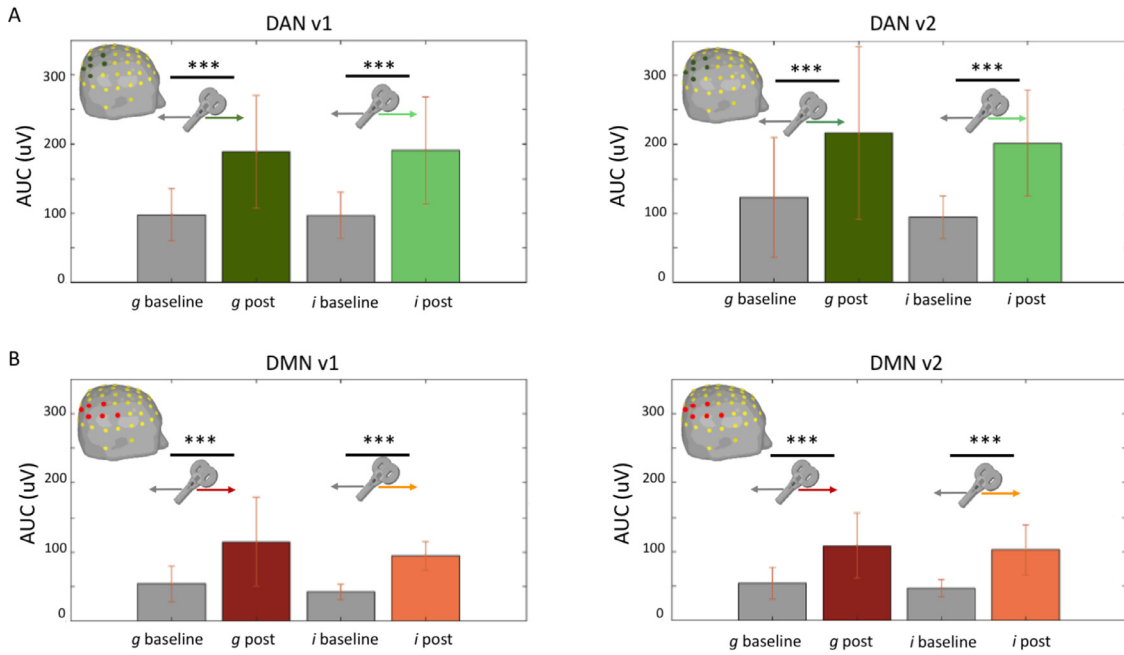
Fig. 5. Induced EEG activity compared to baseline. A. Following stimulation of the DAN, a significant difference from baseline was observed for both the group-based and the individualized condition. Both stimulation scenarios were capable of inducing significantly higher activity (AUC in the 500 ms post pulse) compared to baseline at both test and retest visits. **B.** Similarly for the DMN condition, a significant difference from baseline was observed following both the group-based and the individualized stimulation. A significant difference from baseline was observed across visits. All significant comparisons survived the Bonferroni correction (*** $p<0.0001$). Bars represent standard deviations from the mean. (For interpretation of the references to colour in this figure legend, the reader is referred to the web version of this article.)
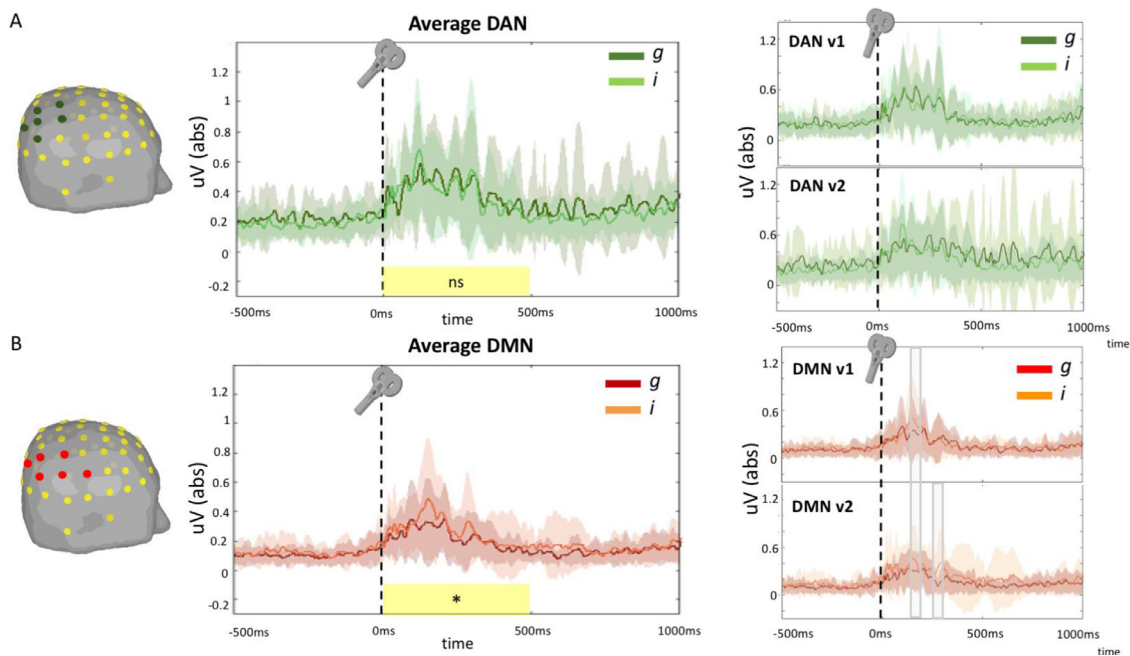

Fig. 6. Efficacy of group-based versus individualized stimulation at the electrode level. The AUC computed from the mean timeseries of the 6 electrodes closer to the stimulation site was compared between the group-derived and individualized targeting condition. **A.** Following stimulation of the DAN, no significant difference was observed between the g and i condition, neither on the overall 500 ms post pulse period, nor at the single temporal window level. **B.** For the DMN stimulation, a significantly higher induced activity was observed following the i compared to the g condition for the whole 500 ms post pulse. Analyses of the single temporal windows revealed a higher induced activity following the i stimulation between 150 and 200 ms post pulse (at both V1 and V2) and between 250 and 300 ms post pulse at V2 only. (For interpretation of the references to colour in this figure legend, the reader is referred to the web version of this article.)
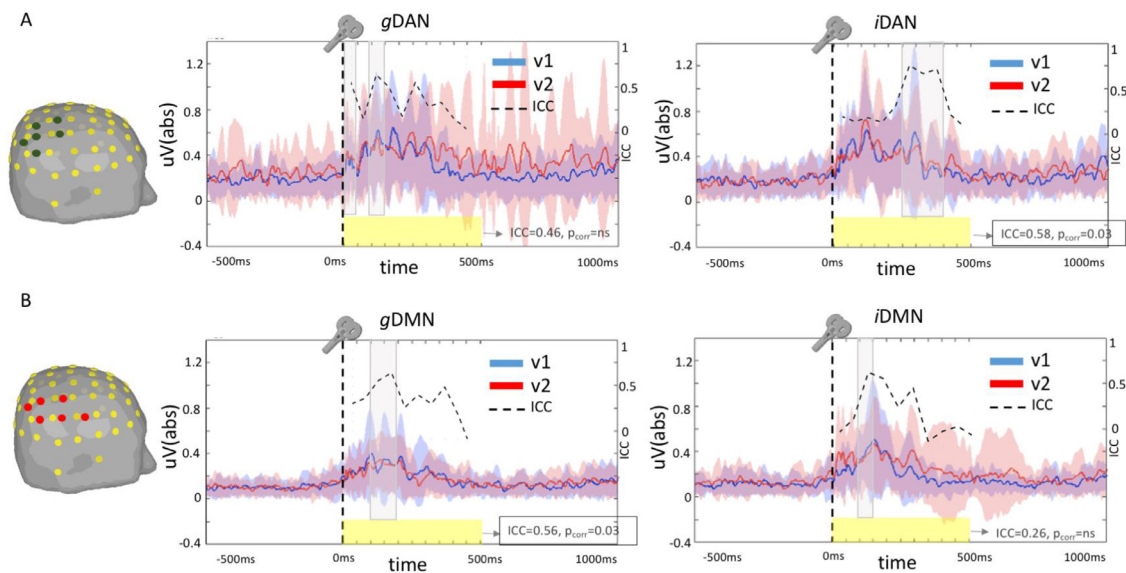
Fig. 7. Reliability of the evoked response following group-derived or individualized stimulation. A. For the DAN, reliability across visits was observed following the *i* stimulation condition. **B.** For the DMN condition, reliability across visits was observed for the *g* stimulation. The yellow shaded area represented the first 500 ms post pulse where the analyses were conducted. The gray shaded area represents the time-windows where reliability of the response surviving the permutation correction was observed. (For interpretation of the references to colour in this figure legend, the reader is referred to the web version of this article.)

Post hoc analyses revealed a significant greater effect following the *i*, compared to the *g*, condition (Mdiff=2.45e-5, $p = 0.03$). When analyses were run considering the single time-windows, a significant effect of stimulation was observed at 150–200 ms post pulse ($F_{(1,21)}$=4.49, $p = 0.045$). Post hoc comparison revealed a greater induced activity by the *i*, compared to the *g*, condition (Mdiff= 5.5e-06, $p = 0.045$). At 250–300 ms, a significant effect of stimulation ($F_{(1,21)}$=7.70, $p = 0.01$) and a significant interaction stimulationXvisit interaction ($F_{(1,21)}$=13.76, $p = 0.001$) were observed. The post hoc analyses revealed greater induced activity following the *i*, compared to the *g*, stimulation (Mdiff= 4.5e-06, $p = 0.01$), which was however present at V2 (Mdiff= 9.4e-06, $p = 0.001$), but not at V1 (Mdiff= −3.3e-07, $p = 0.84$).

The yellow shaded area represented the first 500 ms post pulse where the analyses were conducted. The gray shaded area represents the single time-windows where a significant difference in the activity was observed between the *i* and the *g* stimulation conditions.

3.4. Reliability of the evoked response at the electrode level

Reliability of the induced activity changes was assessed by means of ICC over 1000 permutations, comparing the AUC on the whole 500 ms post pulse, as well as in each single time window. For the DAN condition (Fig. 7A), the reliability of the evoked response following the *g* conditions was observed not to reach the significant threshold (ICC=0.46, p_{corr}=0.1). At the level of the single time-windows, significant reliability was observed in the first 50 ms post pulse (ICC= 0.53, p_{corr}=0.041) and at 100–150 ms (ICC= 0.59, p_{corr}=0.03). Significant ICC values were also observed at 150–200 ms (ICC= 0.44, $p = 0.02$) and 250–300 ms (ICC= 0.51, $p = 0.005$) post pulse, which however did not survive the permutation correction. On the other hand, following the *i* stimulation condition, reliability in the response was observed (ICC=0.58, p_{corr}=0.03). At the level of the single time-windows, high-to-moderate reliability was observed in the 250–300 ms (ICC= 0.77, p_{corr}=0.008), 300–350 ms (ICC= 0.68, $p_{corr} = 0.03$) and 350–400 ms (ICC= 0.73, $p_{corr} = 0.02$) time-windows post pulse.

For the DMN condition (Fig. 7B), reliability in the response across visits was observed for the *g* stimulation (ICC=0.56, p_{corr}=0.03). At the level of the single time-windows, moderate reliability was observed at 100–150 ms (ICC= 0.62, $p_{corr}= 0.047$) and 150–200 ms (ICC= 0.65,

p_{corr}=0.03) post pulse. Significant ICC values following the *g* stimulation were also observed in the 50–100 ms (ICC= 0.36, $p = 0.04$), 250–300 ms (ICC= 0.40, $p = 0.03$) and 350–400 ms (ICC= 0.49, $p = 0.008$) time-windows, which however did not survive the permutation correction. For the *i* condition, the correlation between visits did not reach the significance threshold (ICC=0.26, p_{corr}=0.2). For the single time-windows, reliability was observed at 100–150 ms (ICC= 0.56, p_{corr}= 0.04). Significant ICC values following the *i* stimulation were also observed at 150–200 ms (ICC= 0.55, $p = 0.003$) and 250–300 ms (ICC= 0.45, $p = 0.01$) post pulse, which however did not survive the permutation correction.

3.5. ICA-guided approach

On a small subsample of our participants, an even more personalized approach based on the individual ICA network maps was tested. We were interested in addressing if increased efficacy and reliability were proportional to increased individualization, that is, if substantial differences were present between our *i* and *ica* approach.

At the network level, paired sample t-tests revealed a significant difference from baseline following the *ica* stimulation of the DAN (V1: $t_{(8)}$= −3.57, $p = 0.007$, Hedges' $g = 1.53$; V2: $t_{(8)}$= −4.18, $p = 0.003$, Hedges' $g = 1.2$). However, no significant difference from baseline was observed following the *ica* stimulation of the DMN at V1 ($t_{(6)}$= −1.98, $p = 0.09$, Hedges' $g = 0.86$), whereas it was present at V2 ($t_{(6)}$= −3, $p = 0.02$, Hedges' $g = 1.33$). In this case, only the difference observed at V2 for the DAN stimulation survived the Bonferroni correction (0.05/8; $\alpha = 0.0062$). When the efficacy of the *ica* stimulation was compared to that of the *i* stimulation, no significant differences were observed for the DAN condition (Hedges'g V1= 0.46, Hedges' g V2= 0.11) (Fig. 8A). For the DMN, no significant difference in the induced activity was observed between the *ica* and *i* conditions (Hedges' g V1= 0.44, Hedges' g V2= 0.01). On the other hand, a significant effect of visit was observed at 200–250 ms, ($F_{(1,6)}$=6.63, $p = 0.04$). Post hoc analyses revealed a higher AUC at V2 compared to V1 (Mdiff= 9.5, $p = 0.04$). However, no significant difference was observed between *i* and *ica* stimulation conditions (Fig. 8B).

As for the test-retest reliability, the evoked response in the 500 ms following stimulation of the DAN did not result in a significant corre-
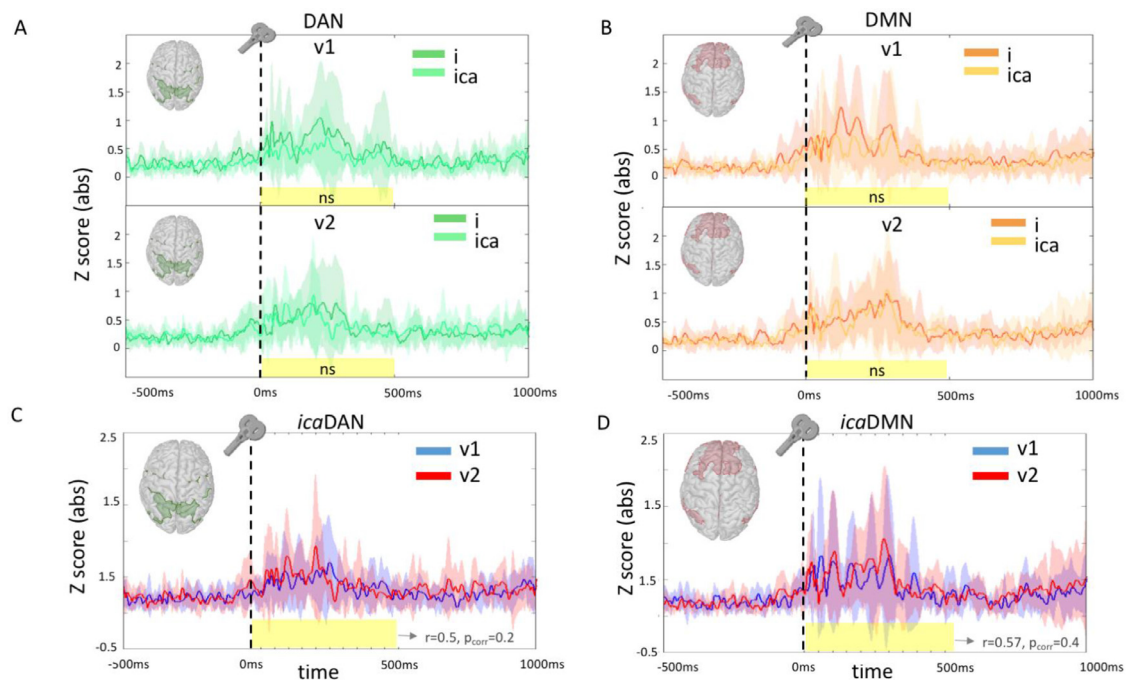
Fig. 8. Efficacy and reliability of *ica* stimulation at the network level. In a small subsample of participants, two individualized approaches (*i* and *ica*) were compared in their efficacy and test-retest reliability. **A.** Stimulation of the DAN resulted in a non-significant difference of the induced effects between the *i* and *ica* conditions at neither the test nor the retest visit. **B.** Similarly for the DMN, a non-significant difference of the induced effects between the *i* and *ica* conditions was observed on the whole 500 ms post pulse. **C.** For the DAN condition, high ICC was observed at 50–100 ms post pulse, which however did not survive permutation correction. **D.** For the DMN condition, the *ica* stimulation resulted in moderate-to-high ICC in the first 50 ms post pulse, as well as at 200–250 ms, 300–350 ms and 350–400 ms post pulse. None of the results however survived permutation correction. The yellow shaded area represented the first 500 ms post pulse where the analyses were conducted. (For interpretation of the references to colour in this figure legend, the reader is referred to the web version of this article.)

lation (ICC=0.5, p_{corr}=0.2) (Fig. 8C). At the level of the single time-windows, a significant ICC was observed at 50–100 ms (ICC=0.77, $p = 0.004$) and 400–450 ms post pulse (ICC= 0.68, $p = 0.01$). However, none of the results survived permutation correction. Similarly for the DMN condition (Fig. 8D), the evoked response in the 500 ms post pulse did not result in a significant correlation (ICC=0.57, p_{corr}=0.4). At the level of the single time-windows, a significant ICC was observed in the first 50 ms post pulse (ICC= 0.71, $p = 0.01$), and in the 200–250 ms (ICC= 0.64, $p = 0.03$), 300–350 ms (ICC= 0.81, $p = 0.004$) and 350–400 ms (ICC= 0.71, $p = 0.02$) time-windows post pulse. However, none of the results survived permutation correction.

When the same analyses were conducted at the electrode level, a significant difference from baseline was observed across visits following the *ica* stimulation of both the DAN (V1: $t_{(8)}= -3.48$, $p = 0.008$, Hedges' $g = 1.06$; V2: $t_{(8)}= -2.46$, $p = 0.04$, Hedges' $g = 1.17$) and the DMN (V1: $t_{(6)}= -2.57$, $p = 0.04$, Hedges' $g = 1.03$; V2: $t_{(6)}= -4.68$, $p = 0.003$, Hedges' $g = 1.7$). However, none of the results survived the Bonferroni correction ($0.05/8$; $\alpha = 0.0062$). To compare the efficacy of *ica* and *i* stimulation conditions, two-way rmANOVAs were run on the 10 participants who underwent both conditions. For the DAN, no difference between the *i* and *ica* approaches was observed (Fig. 9A), neither on the whole 500 ms post pulse (Hedges' g V1= 0.24, Hedges' g V2= 0.3), nor on the single time-windows. For the DMN, no significant effect was observed on the whole 500 ms post pulse (Hedges' g V1= 0.09, Hedges' g V2= 0.62). On the other hand, a significant effect of stimulation was observed between 100 ms and 150 ms post pulse ($F_{(1,6)}$=6.27, $p = 0.046$) (Fig. 9B). Post hoc analyses revealed a greater induced activity of the *i*, compared to the *ica*, stimulation (Mdiff= 7.7e-06, $p = 0.046$). In terms of reliability, the *ica* stimulation of the DAN resulted in a non-significant correlation across visits (ICC=−0.23, p_{corr}=0.6). At the single time-windows level, significant ICC values were observed only at 450–500 ms post pulse (ICC= 0.61, $p = 0.03$), which however did not survive the permutation correction (Fig. 9C). For the DMN condition,

no reliability across visits was instead observed (ICC=−0.01, p_{corr}=0.5) (Fig. 9D).

4. Discussion

The present study aimed at comparing the efficacy and test-retest reliability of the induced TMS response following a single pulse protocol relaying either on i) group-based, generalized target definition or on ii) functionally individualized stimulation sites. To address this query, two networks that are typically functionally anticorrelated were stimulated, respectively the DAN, which is involved in the top-down selection of attentional stimuli and hence represents task-positive manifestations (Corbetta and Shulman, 2002), and the DMN, which represents instead the most well-known task-negative resting state network (Raichle, 2015). At the source level, our results have shown no significant difference in the amount of induced activity in either the DAN, or the DMN, following the two different targeting procedures. As for the reliability of the evoked response across visits, we observed reliable patterns only after individualized stimulation approaches. For the analyses conducted at the network level, interpretation of findings needs to be considered because network maps were used to define the stimulation point as well as masks for the readout of the stimulation. Indeed, our main goal was to compare two TMS hot spots of a given brain network with the assumption that individualized targeting approach will better hit the intended network and thus may lead to more reproducible activation patterns across multiple sessions. Accordingly, please note that, we measured TMS evoked responses at the network level using individualized network maps as our regions of interest. We hypothesized that compared to group based approaches, individualized TMS targeting may better engage the stimulated networks (similar to larger and reproducible MEPs from the motor hot spot) and result in improved reproducibility within and between individuals. Since in this study the network maps were defined based on different approaches, the readout
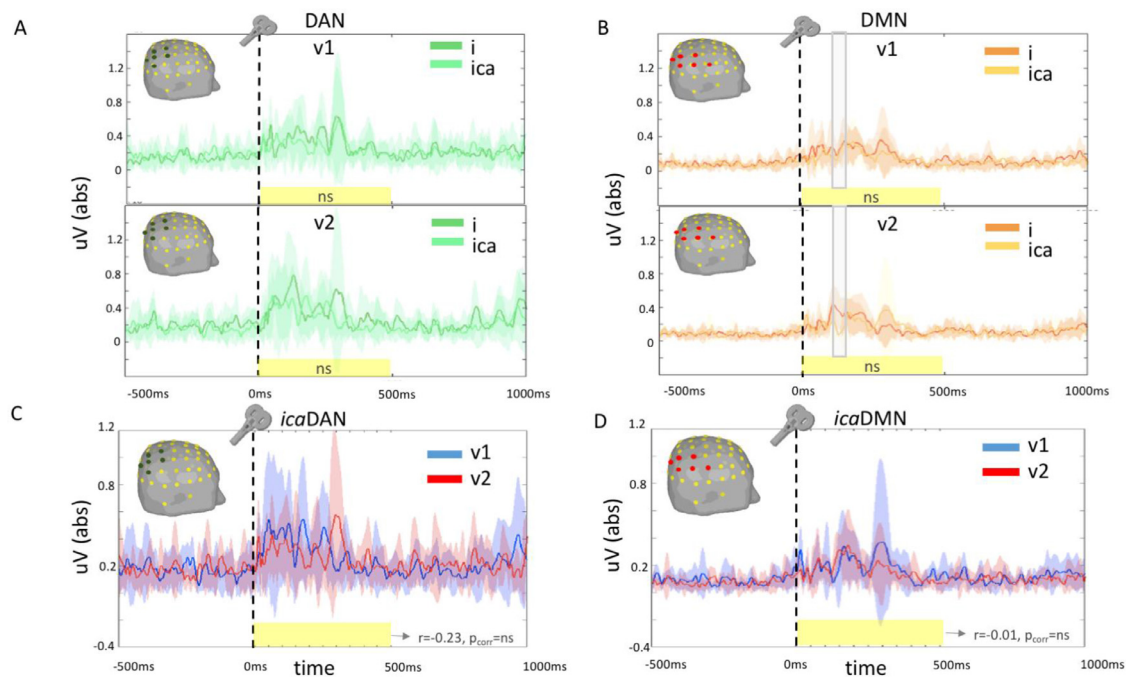
Fig. 9. Efficacy and reliability of *ica* stimulation at the electrode level. In a small subsample of participants, two individualized approaches (*i* and *ica*) were compared in their efficacy and test-retest reliability. **A.** Stimulation of the DAN resulted in a non significant difference of the induced effects between the *i* and *ica* conditions at neither the test nor the retest visits. **B.** Similarly for the DMN, a non significant difference of the induced effects between the *i* and *ica* conditions was observed on the whole 500 ms post pulse; however, a greater induced activity by the *i* conditions was observed between 100 ms and 150 ms post pulse. **C.** The *ica* stimulation of the DAN resulted in poor reliability across visits. **D.** Similarly for the DMN, the ica stimulation showed poor reliability across visits. The yellow shaded area represented the first 500 ms post pulse where the analyses were conducted. The gray shaded area represents the time-windows where reliability of the response surviving the permutation correction was observed. (For interpretation of the references to colour in this figure legend, the reader is referred to the web version of this article.)

for both the group-based and the individualized conditions were specific to each of the stimulation conditions, to ensure that the output signal was measured in the most advantageous scenario for each stimulation approach. The use of networks to inform target selection in TMS studies is not new; rather it has gained a lot of interest in several clinical applications, based on the notion that different network alteration profiles can be appreciated across neurological disorders (Sale et al., 2015; Pini et al., 2018). As a result, several studies have tried to employ TMS to restore healthy network balance (Menardi et al., 2022; Fox et al., 2014), by informing the target selection based on the brain networks maps, which are in turn used as reference for monitoring of the efficacy of the stimulation treatment (Pievani et al., 2016).

When the same analyses were repeated at the electrode level, that is, in the six electrodes surrounding the stimulation site, results were mixed. When the DAN was targeted, reliable response patterns were observed following its individualized stimulation; opposite for the DMN, whereby reliable patterns emerged following its group-based targeting. Indeed, although the individualized approach resulted in a greater induced activity following the stimulation of the DMN, this was observed to be not reliable. In face of this findings, we might conclude that personalization of the stimulation site based on the individual functional topography might not bring substantial differences in the efficacy of the stimulation, as measured based on the quantitative amount of network engagement, but it might have an effect on the reliability of the measured response. In particular, reliability after individualized stimulation protocols was mostly observed at the whole network level, as measured via source analyses, for both the DAN and DMN; and at the electrode space level for the DAN. Notably, the reliability of the TMS evoked potentials (TEPs) has been previously reported in the literature (Lioumis et al., 2009; Kerwin et al., 2018), including recent studies by some of the authors (Ozdemir et al., 2021; Ozdemir et al., 2020). However, differently from these prior studies, we looked at the replicabil-

ity of the induced amount of activity (AUC), rather than at the TEPs waveforms and peaks distribution, showing reliable patterns after the individualized stimulation of the DAN.

A possible interpretation of the different susceptibility of the DAN and DMN to individualized approaches might be imputable to their stability and inter-subject variability as networks. In particular, task-positive functional networks appear to display higher inter-individual variability (Doucet et al., 2019). In a recent study, more than 10 h of resting state and task-fMRI were analyzed to derive high-fidelity individual functional connectomes for the study of the variability of bran networks, proving the DAN to be one of the networks showing the highest inter-subject difference in its topology (Gordon et al., 2017). As pointed out by the authors, a possible source of interindividual differences in the DAN topography is its embedding of middle temporal regions (Fox et al., 2006), which are among the most variable structures of the human brain (Van Essen et al., 2012). In line with this, other task-positive networks have also been proven highly variable, especially in regard of the high subject-specificity of fronto-parietal regions, which play the strongest role in the individual brain fingerprinting (Finn et al., 2015). Indeed, the variability of high order networks appears to be mostly imputable to their embedding of associative regions, which tend to participate to multiple resting state networks, thus increasing their spatial variability (Doucet et al., 2019; Yeo et al., 2014). On the other hand, baseline activity during resting state has been reported generally stable across individuals, as the brain networks with the highest percentage of BOLD signal have been reported to show the least variation (Damoiseaux et al., 2006). This has been reported even in longitudinal studies with older age populations (Beason-Held et al., 2009). Interestingly, the consistency and reliability of the DMN has also been assessed across processing methodologies, for example via effective connectivity analysis (Almgren et al., 2018). In addition, substantial overlap between its spatial distribution has also been observed across neuroimaging modalities,

for example via both resting state functional data and arterial spin labeling (Jann et al., 2015). The fact that the DAN is a more variable neural network compared to the DMN might explain why the individualization of stimulation paradigm is particularly relevant for its reliable targeting, as shown in the present study.

The knowledge that different brain networks might have different susceptibility to the individualization of their targeting is of great importance. In particular, it might guide future efforts in determining when personalized interventions are the most desirable option. However, the use of personalized protocols necessarily increases the cost and feasibility of their application, such as that the higher the required degree of personalization, the more demanding the paradigm becomes. For this reason, in a small subsample of participants, we compared two different degrees of individualized solutions to determine if increased personalization would result in differences in the efficacy / reliability of the TMS-response, or if a plateau is instead achieved. In the first individualized approach, the seed region was iteratively determined, allowing to move from atlas-based regions (as used in the group-based approach) to individual, data-driven, networks' seeds. In the second, even more personalized approach, networks definition was entirely data driven from individualized ICA-derived network maps over three fMRI runs. Interestingly, for both networks tested, we did not observe significant differences in either the amount of induced activity post-pulse, or the reliability across visits of such response. Although highly preliminary, due to the limited number of participants tested in these sub-analyses, our results suggest that a first level of individualization might be sufficient in reaching satisfactory reliability estimates, while limiting the burden of more advanced solutions. Still, based on our findings, the option of personalized interventions might be particularly relevant in protocols aiming at targeting highly variable cortical networks, and less instead for those proven to be more stable across individuals. For example, although not directly tested in this study, based on prior literature findings we can estimate that other highly stable networks, such as the Visual and the Sensorimotor networks, would also not substantially benefit from personalized stimulation approaches, as they show highly consistent anatomic morphology and highly coherent functional connectivity patterns (Doucet et al., 2019).

The present study only deals with the reliability of the EEG response evoked by a single TMS pulse. Nevertheless, we might argue that single-pulse results demonstrating increased reliability of TMS-evoked activity over time with individualized targeting might suggest that repetitive protocols (rTMS) sessions applied to the individualized target might also more reliably activate a consistent network, and thus be more likely to achieve a modulatory effect. However, this is a hypothesis that clearly needs validation. Although reliability does not necessarily translate into greater efficacy, it has been previously pointed out that reproducible TMS-EEG responses are not only valuable in understanding cortical excitability itself, but also in tracking more precisely the physiological effects of repeated pulse delivery on the brain (Lioumis et al., 2009). The personalization of rTMS protocols is indeed becoming a priority in current research studies as an approach aimed at increasing the number of treatment responders (Schoisswohl et al., 2021; Cash et al., 2021; Cocchi and Zalesky, 2018). Prior investigations have observed the strongest behavioral effect sizes in studies employing personalized TMS targeting based on fMRI connectivity, compared to studies employing targeting based on structural, population-derived coordinates or EEG electrodes positions (Sack et al., 2009). Similarly, power analyses revealed the need of the least amount of participants to observe behavioral changes in fMRI guided TMS compared to all other targeting methodologies (Sack et al., 2009).

In this direction, future studies should further address the extent and validity of these findings, possibly considering more advanced personalized techniques, as well as their reliability over several months. Indeed, we cannot exclude that more sophisticated personalized stimulation models would increase the efficacy and reliability of TMS-induced activity, which we were not able to test in the present investigation. An example of an additional level of complexity that future studies should address is the tailoring of stimulation considering the individual underlying brain state. Indeed, the identification of the stimulation site based on the individual functional connectome is highly subjective to the brain state happening when it is first computed, which might not reflect the same brain state at the time of stimulation. One possible solution could be that of employing the same priming method, for example through the execution of a given cognitive task, at the time of neuroimaging data acquisition and at the following stimulation visit to try maintain consistency of the brain state occurring across visits. However, because this additional setting requirement would further stress the cost / benefits ratio, additional care should be paid in defining a trade-off between efficiency and practicality of such interventions. Still, the core of these approaches remains that of looking into individual specifics while avoiding to treat the acquired data in a group-generalized fashion, which necessarily limits their quality, detail and ultimate usefulness, overall failing to report unique connectivity ensembles (Gordon et al., 2017; Laumann et al., 2015). Furthermore, since our results show high sensitivity to the individualization of the stimulation target for reliable DAN engagement, future studies might employ TMS protocols for network parcellation purposes at the single subject level, which prior studies have pointed out as a crucial step in the tailoring of personalized medicine approaches (Wang et al., 2015). Finally, the present study was conducted on young, healthy individuals with normal brain patterns. It is therefore hard to generalize the present findings to older adults or patients with various brain diseases in whom pathology and/or age may be associated with alteration of functional networks and higher inter-subject variability. It is noteworthy though that in such scenarios, the personalization of interventions would be of even greater importance (Ginsburg and Phillips, 2018; Hampel et al., 2019).

5. Conclusions

Reliability of TMS protocols is highly debated. However, test-retest reproducibility might be improved by the individualization of stimulation sites based on the participant's functional connectivity profile. Notably, individualized protocols yield different success rates depending on the network stimulated: personalized sites are of greater importance for networks that show high inter-subject variability (e.g., the DAN), but might be less relevant for relatively stable and consistent networks (e.g., the DMN).

Author Declaration

We wish to draw the attention of the Editor to the following facts which may be considered as potential conflicts of interest and to significant financial contributions to this work:

A. Pascual-Leone is a co-founder of Linus Health and TI Solutions AG; serves on the scientific advisory boards for Starlab Neuroscience, Magstim Inc., Hearts Radiant, TetraNeuron and MedRhythms; and is listed as an inventor on several issued and pending patents on methods and applications for noninvasive brain stimulation, and the real-time integration of noninvasive brain stimulation with electroencephalography and magnetic resonance imaging. None of these companies or interests influenced in any way the work reported.

All other authors report no conflict of interest.

We confirm that the manuscript has been read and approved by all named authors and that there are no other persons who satisfied the criteria for authorship but are not listed. We further confirm that the order of authors listed in the manuscript has been approved by all of us.

We confirm that we have given due consideration to the protection of intellectual property associated with this work and that there are no impediments to publication, including the timing of publication, with respect to intellectual property. In so doing we confirm that we have followed the regulations of our institutions concerning intellectual property.

We further confirm that any aspect of the work covered in this manuscript that has involved either experimental animals or human patients has been conducted with the ethical approval of all relevant bodies and that such approvals are acknowledged within the manuscript.

We understand that the Corresponding Author is the sole contact for the Editorial process (including Editorial Manager and direct communications with the office). He/she is responsible for communicating with the other authors about progress, submissions of revisions and final approval of proofs. We confirm that we have provided a current, correct email address which is accessible by the Corresponding Author and which has been configured to accept email from: arianna.menardi@gmail.com

Data sharing

Raw and preprocessed data are available at Berenson-Allen Center for Noninvasive Brain Stimulation site (http://www.tmslab.org/netconlab.php).

Declaration of Competing Interest

A. Pascual-Leone is a co-founder of Linus Health and TI Solutions AG; serves on the scientific advisory boards for Starlab Neuroscience, Magstim Inc., Hearts Radiant, TetraNeuron and MedRhythms; and is listed as an inventor on several issued and pending patents on methods and applications for noninvasive brain stimulation, and the real-time integration of noninvasive brain stimulation with electroencephalography and magnetic resonance imaging. None of these companies or interests influenced in any way the work reported.

Credit authorship contribution statement

Arianna Menardi: Formal analysis, Writing – original draft. **Recep A. Ozdemir:** Formal analysis, Data curation, Writing – review & editing. **Davide Momi:** Data curation, Writing – review & editing. **Ehsan Tadayon:** Data curation, Writing – review & editing. **Pierre Boucher:** Data curation, Writing – review & editing. **Antonino Vallesi:** Writing – review & editing. **Alvaro Pascual-Leone:** Conceptualization, Funding acquisition, Supervision, Writing – review & editing. **Mouhsin M. Shafi:** Conceptualization, Funding acquisition, Supervision, Writing – review & editing. **Emiliano santarnecchi:** Conceptualization, Funding acquisition, Supervision, Writing – review & editing.

Data Availability

Data will be made available on request.

Supplementary materials

Supplementary material associated with this article can be found, in the online version, at doi:10.1016/j.neuroimage.2022.119714.

References

Almgren, H., Van de Steen, F., Kuhn, S., Razi, A., Friston, K.J., Marinazzo, D., 2018. Variability and reliability of effective connectivity within the core default mode network: a multi-site longitudinal spectral DCM study. Neuroimage 183, 757–768. doi:10.1016/j.neuroimage.2018.08.053.

Beason-Held, L.L., Kraut, M.A., Resnick, S.M., 2009. Stability of Default-Mode Network Activity in the Aging Brain. Brain Imaging Behav. 3, 123–131. doi:10.1007/s11682-008-9054-z.

Belardinelli, P., Biabani, M., Blumberger, D.M., Bortoletto, M., Casarotto, S., David, O., et al., 2019. Reproducibility in TMS–EEG studies: a call for data sharing, standard procedures and effective experimental control. Brain Stimul. 12, 787–790. doi:10.1016/j.brs.2019.01.010.

Cash, R.F.H., Cocchi, L., Lv, J., Wu, Y., Fitzgerald, P.B., Zalesky, A., 2021. Personalized connectivity-guided DLPFC-TMS for depression: advancing computational feasibility, precision and reproducibility. Hum. Brain Mapp. 42, 4155–4172. doi:10.1002/hbm.25330.

Cash, R.F.H., Weigand, A., Zalesky, A., Siddiqi, S.H., Downar, J., Fitzgerald, P.B., et al., 2020. Using Brain Imaging to Improve Spatial Targeting of Transcranial Magnetic Stimulation for Depression. Biol. Psychiatry doi:10.1016/j.biopsych.2020.05.033, In Press:12.

Cocchi, L., Zalesky, A., 2018. Personalized Transcranial Magnetic Stimulation in Psychiatry. Biol. Psychiatry 3, 731–741. doi:10.1016/j.bpsc.2018.01.008.

Connolly, K.R., Helmer, A., Cristancho, M.A., Cristancho, P., O'Reardon, J.P., 2012. Effectiveness of Transcranial Magnetic Stimulation in Clinical Practice Post-FDA Approval in the United States: results Observed With the First 100 Consecutive Cases of Depression at an Academic Medical Center. J. Clin. Psychiatry 73, 567–573. doi:10.4088/JCP.11m07413.

Corbetta, M., Shulman, G.L., 2002. Control of goal-directed and stimulus-driven attention in the brain. Nat. Rev. Neurosci. 3, 201–215. doi:10.1038/nrn755.

Corp, D.T., Bereznicki, H.G.K., Clark, G.M., Youssef, G.J., Fried, P.J., Jannati, A., et al., 2021. Large-scale analysis of interindividual variability in single and paired-pulse TMS data. Clin. Neurophysiol. doi:10.1016/j.clinph.2021.06.014.

Damoiseaux, J.S., Rombouts, S a.RB, Barkhof, F., Scheltens, P., Stam, C.J., Smith, S.M., et al., 2006. Consistent resting-state networks across healthy subjects. Proc. Natl Acad. Sci. 103, 13848–13853. doi:10.1073/pnas.0601417103.

Delorme, A., Makeig, S., 2004. EEGLAB: an open source toolbox for analysis of single-trial EEG dynamics including independent component analysis. J. Neurosci. Methods 134, 9–21. doi:10.1016/j.jneumeth.2003.10.009.

Doucet, G.E., Lee, W.H., Frangou, S., 2019. Evaluation of the spatial variability in the major resting-state networks across human brain functional atlases. Hum. Brain Mapp. 40, 4577–4587. doi:10.1002/hbm.24722.

Finn, E.S., Shen, X., Scheinost, D., Rosenberg, M.D., Huang, J., Chun, M.M., et al., 2015. Functional connectome fingerprinting: identifying individuals using patterns of brain connectivity. Nat. Neurosci. 18, 1664–1671. doi:10.1038/nn.4135.

Fox, M.D., Buckner, R.L., Liu, H., Chakravarty, M.M., Lozano, A.M., Pascual-Leone, A., 2014. Resting-state networks link invasive and noninvasive brain stimulation across diverse psychiatric and neurological diseases. Proc. Natl. Acad. Sci. U.S.A. 111, E4367. doi:10.1073/pnas.1405003111.

Fox, M.D., Corbetta, M., Snyder, A.Z., Vincent, J.L., Raichle, M.E., 2006. Spontaneous neuronal activity distinguishes human dorsal and ventral attention systems. Proc. Natl. Acad. Sci. 103, 10046–10051. doi:10.1073/pnas.0604187103.

Fox, M.D., Hesheng, L., Pascual-Leone, A., 2013. Identification of reproducible individualized targets for treatment of depression with TMS based on intrinsic connectivity. Neuroimage 66, 151–160. doi:10.1016/j.neuroimage.2012.10.082.

Ginsburg, G.S., Phillips, K.A., 2018. Precision medicine: from science to value. Health Aff. doi:10.1377/hlthaff.2017.1624.

Gordon, E.M., Laumann, T.O., Gilmore, Adrian W., Newbold, D.J., Greene, D.J., Berg, J.J., et al., 2017. Precision functional mapping of individual human brains. Neuron 95, 791–807. doi:10.1016/j.neuron.2017.07.011, e7.

Hallett, M., 2000. Transcranial magnetic stimulation and the human brain. Nature 406, 147–150. doi:10.1038/35018000.

Hampel, H., Vergallo, A., Perry, G., Lista, S., 2019. Initiative (APMI) the APM. The Alzheimer Precision Medicine Initiative. J. Alzheimers Dis. 68, 1–24. doi:10.3233/JAD-181121.

Huerta, P.T., Volpe, B.T., 2009. Transcranial magnetic stimulation, synaptic plasticity and network oscillations. J. NeuroEngin. Rehabil. 6, 1–10. doi:10.1186/1743-0003-6-7.

Jann, K., Gee, D.G., Kilroy, E., Schwab, S., Smith, R.X., Cannon, T.D., et al., 2015. Functional connectivity in BOLD and CBF data: similarity and reliability of resting brain networks. Neuroimage 106, 111–122. doi:10.1016/j.neuroimage.2014.11.028.

Kerwin, L.J., Keller, C.J., Wu, W., Narayan, M., Etkin, A., 2018. Test-retest reliability of transcranial magnetic stimulation EEG evoked potentials. Brain Stimul. 11, 536–544. doi:10.1016/j.brs.2017.12.010.

Koo, T.K., Li, M.Y., 2016. A guideline of selecting and reporting intraclass correlation coefficients for reliability research. J. Chiropr. Med. 15, 155. doi:10.1016/j.jcm.2016.02.012.

Laumann, T., Gordon, E.M., Adeyemo, B., Snyder, A.Z., Jun Joo, S., Chen, M.-.Y., et al., 2015. Functional system and areal organization of a highly sampled individual human brain. Neuron 87, 657–670. doi:10.1016/j.neuron.2015.06.037.

Lefaucheur, J.P., Aleman, A., Baeken, C., Benninger, D.H., Brunelin, J., Di Lazzaro, V., et al., 2020. Evidence-based guidelines on the therapeutic use of repetitive transcranial magnetic stimulation (rTMS): an update (2014–2018). Clin. Neurophysiol. 131, 474–528. doi:10.1016/j.clinph.2019.11.002.

Lioumis, P., Kičić, D., Savolainen, P., Mäkelä, J.P., Kähkönen, S., 2009. Reproducibility of TMS—Evoked EEG responses. Hum. Brain Mapp. 30, 1387–1396. doi:10.1002/hbm.20608.

Lopez-Alonso, V., Cheeran, B., Rio-Rodrigues, D., Fernandez-del-Olmo, M., 2014. Inter-individual variability in response to non-invasive brain stimulation paradigms. Brain Stimul. 7, 372–380. doi:10.1016/j.brs.2014.02.004.

Lynch, C.J., Elbau, I.G., Ng, T.H., Wolk, D., Zhu, S., Ayaz, A., et al., 2022. Automated optimization of TMS coil placement for personalized functional network engagement. Neuron doi:10.1016/j.neuron.2022.08.012, In press.

McGraw, K.O., Wong, S.P., 1996. Forming inferences about some intraclass correlation coefficients. Psychol. Methods 1, 30–46.

Menardi, A., Rossi, S., Koch, G., Hampel, H., Vergallo, A., Nitsche, M.A., et al., 2022. Toward noninvasive brain stimulation 2.0 in Alzheimer's disease. Ageing Res. Rev. 75, 101555. doi:10.1016/j.arr.2021.101555.

Momi, D., Ozdemir, R.A., Tadayon, E., Boucher, P., Shafi, M.M., Pascual-Leone, A., et al., 2021. Network-level macroscale structural connectivity predicts propagation of transcranial magnetic stimulation. Neuroimage 229, 117698. doi:10.1016/j.neuroimage.2020.117698.

Moreno-Ortega, M., Kangarlu, A., Lee, S., Perera, T., Kangarlu, J., Palomo, T., et al., 2020. Parcel-guided rTMS for depression. Transl. Psych.. 10, 1–6. doi:10.1038/s41398-020-00970-8.

Nestor, S.M., Blumberger, D.M., 2020. Mapping symptom clusters to circuits: toward personalizing TMS targets to improve treatment outcomes in depression. Am. J. Psychiatry doi:10.1176/appi.ajp.2020.20030271.

Nettekoven, C., Volz, L.J., Leimbach, M., Pool, E.-.M., Rehme, A.K., Eickhoff, S.B., et al., 2015. Inter-individual variability in cortical excitability and motor network connectivity following multiple blocks of rTMS. Neuroimage 118, 209–218. doi:10.1016/j.neuroimage.2015.06.004.

Oathes, D.J., Zimmerman, J.P., Duprat, R., Japp, S.S., Scully, M., Rosenberg, B.M., et al., 2021. Resting fMRI-guided TMS results in subcortical and brain network modulation indexed by interleaved TMS/fMRI. Exp. Brain Res. 239, 1165–1178. doi:10.1007/s00221-021-06036-5.

Ozdemir, R.A., Tadayon, E., Boucher, P., Momi, D., Karakhanyan, K.A., Fox, M.D., et al., 2020. Individualized perturbation of the human connectome reveals reproducible biomarkers of network dynamics relevant to cognition. Proc. Natl. Acad. Sci., 201911240 doi:10.1073/pnas.1911240117.

Ozdemir, R.A., Tadayon, E., Boucher, P., Sun, H., Momi, D., Ganglberger, W., et al., 2021. Cortical responses to noninvasive perturbations enable individual brain fingerprinting. Brain Stimul. 14, 391–403. doi:10.1016/j.brs.2021.02.005.

Pievani, M., Pini, L., Cappa, S.F., Frisoni, G.B., 2016. Brain networks stimulation in dementia: insights from funcional imaging. Curr. Opin. Neurol. 29, 756–762. doi:10.1097/WCO.0000000000000387.

Pini, L., Manenti, R., Cotelli, M., Pizzini, F.B., Frisoni, G.B., Pievani, M., 2018. Noninvasive brain stimulation in dementia: a complex network story. NDDS 18, 281–301. doi:10.1159/000495945.

Raichle, M.E., 2015. The brain's default mode network. Annu. Rev. Neurosci. 38, 433–447. doi:10.1146/annurev-neuro-071013-014030.

Rogasch, N.C., Sullivan, C., Thompson, R.H., Rose, N.S., Bailey, N., Fitzgerald, P.B., et al., 2017. Analysing concurrent transcranial magnetic stimulation and electroencephalographic data: a review and introduction to the open-source TESA software. Neuroimage 147, 934–951. doi:10.1016/j.neuroimage.2016.10.031.

Sack, A.T., Cohen Kadosh, R., Schuhmann, T., Moerel, M., Walsh, V., Goebel, R., 2009. Optimizing functional accuracy of TMS in cognitive studies: a comparison of methods. J. Cogn. Neurosci. 21, 207–221. doi:10.1162/jocn.2009.21126.

Sale, M.V., Mattingley, J.B., Zalesky, A., Cocchi, L., 2015. Imaging human brain networks to improve the clinical efficacy of non-invasive brain stimulation. Neurosci. Biobehav. Rev. 57, 187–198. doi:10.1016/j.neubiorev.2015.09.010.

Schoisswohl, S., Langguth, B., Hebel, T., Abdelnaim, M.A., Volberg, G., Schecklmann, M., 2021. Heading for personalized rTMS in Tinnitus: reliability of Individualized Stimulation Protocols in Behavioral and Electrophysiological Responses. J. Pers. Med. 11, 536. doi:10.3390/jpm11060536.

Schwedt, T.J., Vargas, B., 2015. Neurostimulation for treatment of migraine and cluster headache. Pain Med. 16, 1827–1834. doi:10.1111/pme.12792.

Siddiqi, S.H., Taylor, S.F., Cooke, D., Pascual-Leone, A., George, M.S., Fox, M.D., 2020. Distinct symptom-specific treatment targets for circuit-based neuromodulation. Am. J. Psychiatry doi:10.1176/appi.ajp.2019.19090915.

Stultz, D.J., Osburn, S., Burns, T., Pawlowska-Wajswol, S., Walton, R., 2020. Transcranial Magnetic Stimulation (TMS) Safety with Respect to Seizures: a Literature Review. Neuropsychiatr. Dis. Treat 16, 2989. doi:10.2147/NDT.S276635.

Tadel, F., Baillet, S., Mosher, J.C., Pantazis, D., Leahy, R.M., 2011. Brainstorm: a User-Friendly Application for MEG/EEG Analysis. Comput. Intell. Neurosci. 2011, 1–13. doi:10.1155/2011/879716.

Terranova, C., Rizzo, V., Cacciola, A., Chillemi, G., Calamuneri, A., Milardi, D., et al., 2019. Is there a future for non-invasive brain stimulation as a therapeutic tool? Front. Neurol. 0. doi:10.3389/fneur.2018.01146.

Valero-Cabrè, A., Amengual, J.L., Stengel, C., Pascual-Leone, A., Coubard, O.A., 2017. Transcranial magnetic stimulation in basic and clinical neuroscience: a comprehensive review of fundamental principles and novel insights. Neurosci. Biobehav. Rev. 83, 381–404. doi:10.1016/j.neubiorev.2017.10.006.

Van Essen, D.C., Glasser, M.F., Dierker, D.L., Harwell, J., Coalson, T., 2012. Parcellations and hemispheric asymmetries of human cerebral cortex analyzed on surface-based atlases. Cereb. Cortex 22, 2241–2262. doi:10.1093/cercor/bhr291.

Wang, D., Buckner, R.L., Fox, M.D., Holt, D.J., Holmes, A.J., Stoecklein, S., et al., 2015. Parcellating cortical functional networks in individuals. Nat. Neurosci. 18, 1853–1860. doi:10.1038/nn.4164.

Yeo, B.T.T., Krienen, F.M., Chee, M.W.L., Buckner, R.L., 2014. Estimates of segregation and overlap of functional connectivity networks in the human cerebral cortex. Neuroimage 88, 212–227. doi:10.1016/j.neuroimage.2013.10.046.

Yeo, B.T.T., Krienen, F.M., Sepulcre, J., Sabuncu, M.R., Lashkari, D., Hollinshead, M., et al., 2011. The organization of the human cerebral cortex estimated by intrinsic functional connectivity. J. Neurophysiol. doi:10.1152/jn.00338.2011.

Young, J.R., Galla, J.T., Appelbaum, L.G., 2021. Transcranial Magnetic Stimulation Treatment for Smoking Cessation: an Introduction for Primary Care Clinicians. Am. J. Med. 134, 1339–1343. doi:10.1016/j.amjmed.2021.06.037.